

## Trapping of DNA by Thermophoretic Depletion and Convection

Dieter Braun\* and Albert Libchaber

Center for Studies in Physics and Biology, Rockefeller University, New York, New York 10021

(Received 2 May 2002; published 14 October 2002)

Thermophoresis depletes DNA from a heated spot. We quantify for the first time the thermal diffusion constant  $D_T = 0.4 \times 10^{-8} \text{ cm}^2/\text{s K}$  for DNA, using fluorescent dyes and laser heating. For 5 kbp DNA we extrapolate a 1000-fold depletion from a temperature difference of 50 K. Surprisingly, convection generated by the same heating can turn the depletion into trapping of DNA. Trapped DNA can form point geometries  $20 \mu\text{m}$  in diameter with more than 1000-fold enhanced concentrations. The accumulation is driven only by temperature gradients and offers a new approach to biological microfluidics and replicating systems in prebiotic evolution.

DOI: 10.1103/PhysRevLett.89.188103

PACS numbers: 87.15.He, 82.70.Dd, 82.60.Lf

Thermophoresis [1,2] repels particles and molecules along temperature gradients from a heated spot. It is often considered a small effect. Yet, as we measure the thermophoretic diffusion constant of DNA, we extrapolate that a temperature difference of 50 K leads to a 1000-fold depletion of 5 kbp DNA. Interestingly, with convection, this depletion can be turned into an accumulation. This is not expected since convection normally mixes a solution towards equal concentration. In given conditions, the same heat source will drive convection and repel DNA into a stable stagnation point against a colder surface. We suspect that such a synergistic double result of heating is quite general and can be found in many different geometries.

We speculate that the trapping from thermophoresis and convection could provide an efficient mechanism to catalyze replicating systems of prebiotic evolution in hot porous stones. Models of prebiotic evolution are puzzled by the kinetic gap due to low molecule concentration in models of self-replication [3,4], rendering the process much too slow to explain the prebiotic evolution of organisms in a time window of  $500 \times 10^6$  years [4]. Second, one should consider that most molecular analysis in biochemistry is based on electrophoresis which is difficult to miniaturize. Micromanipulation techniques like optical tweezing [5] can trap only large, collapsed DNA, and dielectrophoresis [6] needs sophisticated electrode/barrier geometries. Thermophoresis, on the other hand, may yield an elegant new approach to purification and analysis of biomolecules.

Thermophoresis is also called thermodiffusion or the Ludwig [1]–Soret [2] effect and describes the particle movement due to a temperature gradient, typically from hot to cold. It is most efficient for aerosols and dust particles in air. It can also be found for particles or molecules in solution, but its theoretical basis there is still unclear [7–10], especially in the less studied case of aqueous solutions. Thermophoresis can be measured with various techniques [11–15] and is applied in polymer separation [14,15]. Thermophoretic depletion intensifies by convection in long Clusius accumulation tubes [16,17].

*Thermophoresis of DNA.*—For the first time, we measure the thermophoresis of DNA by monitoring the temperature of the buffer and the concentration of DNA both by fluorescence (Fig. 1). We locally heat water with an infrared laser by  $\Delta T = 2.3 \text{ K}$  [Fig. 1(a)] and measure from the fluorescence intensity the subsequent DNA concentration decrease of  $c/c_0 = 73\%$  due to thermophoretic repulsion [Fig. 1(c)].

Plasmid-sized DNA (5.6 kbp, 50 nM, plasmid pET11D) was stained with SYBR-Green ( $10 \times$ , temperature dependence near  $20^\circ\text{C}$  is  $-0.96\% \text{ K}^{-1}$ , S-7563, Molecular Probes) in an aqueous buffer (10 mM TRIS, pH 7.8). We heat the buffer modestly in a  $25 \mu\text{m}$  thin chamber (spacer material SSP-M213, GE Silicones, chamber walls PDMS, Sylgard 184, Dow Corning) with an infrared laser with 0.13 mW [18]. The temperature increase is  $\Delta T = 2.3^\circ\text{C}$  as imaged using the nearly linear

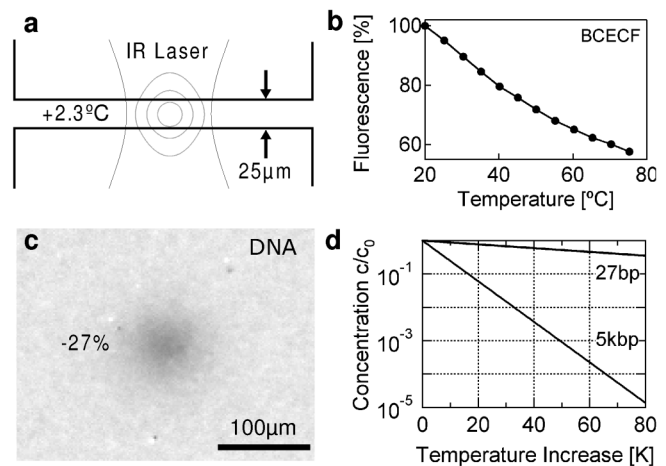


FIG. 1. Thermophoresis of DNA. (a),(b) The temperature in a thin chamber is raised by 2.3 K with infrared heating as measured by the fluorescence of BCECF. (c) DNA (5.6 kbp) is repelled along the gradients by thermophoresis. A concentration drop of  $-27\%$  is imaged by the DNA stain SYBR. (d) Extrapolated from Eq. (2), a more than 1000-fold depletion at a temperature increase of 50 K is expected.

temperature-sensitive fluorescence of BCECF (200  $\mu\text{M}$ , temperature sensitivity near 20  $^{\circ}\text{C}$  is  $-0.95\% \text{ K}^{-1}$ , B-1151, Molecular Probes) as shown in Fig. 1(b). The temperature distribution is checked against a 2D numerical simulation. It is shown in grey equithermal lines with a spacing of 0.5 K. The gradient is mostly parallel to the chamber walls due to the low conducting PDMS chamber material [Fig. 1(a)]. Therefore the optical averaging across the chamber yields a small error.

Thermophoresis in a resting binary fluid is described phenomenologically with Onsager's theory [9]

$$j = -D[Vc + S_T c(1 - c)\nabla T] \quad (1)$$

with the current density  $j$ , the concentration  $c$  given as the molar fraction of DNA to water, the diffusion coefficient  $D$  of DNA in water, the concentration and temperature gradient  $\nabla c$ ,  $\nabla T$ , and the dimensional Soret coefficient  $S_T = D_T/D$  with  $D_T$  the thermal diffusion coefficient of DNA in water. It can be integrated in steady state under negligible convection using the boundary conditions  $c_0$ ,  $T_0$  and the approximations  $c$ ,  $c_0 \ll 1$ .

$$\frac{c}{c_0} = e^{-S_T(T-T_0)}. \quad (2)$$

From the measured  $c/c_0 = 73\%$  and  $\Delta T = 2.3 \text{ K}$  at  $T = 24 \text{ }^{\circ}\text{C}$ , we estimate  $S_T = 0.14 \text{ K}^{-1}$  from [Eq. (2)] using the approximation of a constant temperature profile in the cross section. To measure the diffusion coefficient of DNA, we track the width of the concentration dip with a Gaussian fit after switching off the heating and find  $D = 3.4 \times 10^{-8} \text{ cm}^2/\text{s}$ , consistent with literature [19]. We thus deduce a thermal diffusion coefficient of  $D_T = 0.4 \times 10^{-8} \text{ cm}^2/\text{s K}$ . This value is lower than typical thermal diffusion coefficients of polymers in nonaqueous solutions [15,20]. We have also measured shorter DNA [21]. This thermal diffusion coefficient implies that with a temperature difference of 50 K, we find a more than 1000-fold depletion for 5.6 kbp DNA [Fig. 1(d)].

**Mechanism of thermophoretic trapping.**—Trapping can be found after doubling the chamber thickness to 50  $\mu\text{m}$ , using cooling glass cover slips and increasing the heating power to 10 mW (Fig. 2). Thermal convection is then greatly enhanced and gives rise to an accumulation of DNA at the lower surface of the chamber near the heating spot. The concentration of DNA is again monitored by fluorescence, and we show images before heating [Fig. 2(b)], after heating for 10 s [Fig. 2(c)], and in steady state after 60 s [Fig. 2(d)]. The repulsion by thermophoresis is now much stronger [Fig. 2(c) vs Fig. 1(b)]. Shortly after repulsion, the DNA is accumulated in a ring geometry at the bottom of the chamber by a synergistic combination of four phenomena [Fig. 2(d)]: (1) DNA is repelled from the heated center by lateral thermophoresis. (2) Convection breaks the symmetry and transports the repelled DNA downwards, while upward convection occurs in the depleted center. (3) Axial thermophoresis pins the DNA with high temperature gradients towards the cooling glass most efficiently in the slow flow near the

central stagnation point. (4) The DNA brought by convection is laterally repelled by the edges of the Gaussian heating spot into a ring of accumulation. To summarize, the trapping is the result of an interplay of convection and thermophoresis which are both induced by temperature gradients. We will substantiate the model in the following paragraphs.

We estimate the DNA concentration in the accumulated ring. Fluorescence intensity  $I$  at the ring when compared with the initial fluorescence intensity  $I_0$  yields  $I/I_0 = 1.3$ . The intensities are averages over the chamber thickness as we determine the Gaussian focus depth  $\sigma = 680 \mu\text{m}$  by focusing through a 25  $\mu\text{m}$  thick chamber [Fig. 3(b), objective  $32\times$ , NA = 0.4, 440850, Zeiss). From movements of 1  $\mu\text{m}$  beads (F-13081, Molecular Probes), we find an advection speed of 10  $\mu\text{m}/\text{s}$  at a distance of 5  $\mu\text{m}$  from the bottom surface near the center. Dividing the diffusion constant of DNA by above velocity yields a length scale of 0.3  $\mu\text{m}$ . This should be seen only as an order of magnitude estimate, since the flow characteristics are difficult to assess. If we estimate a height of the accumulation to be  $d = 1 \mu\text{m}$  and conservatively

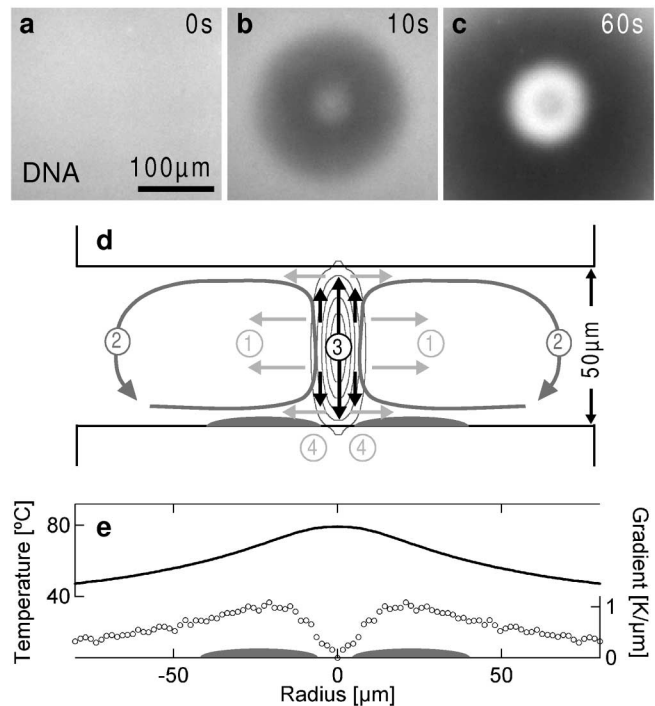


FIG. 2. Mechanism of thermophoretic trapping of DNA. (a) Image of stained DNA before heating. (b) Thermophoresis from central heating first repels DNA laterally. (c) Thermophoresis and toroidal convection trap DNA in the center toward the lower chamber wall in a ring geometry. The concentration enhancement is 13-fold. (d) The mechanism of thermophoretic trapping in the center is an interplay of lateral thermophoresis (1), (4) and axial thermophoresis (3) with convection (2). (e) The ring geometry is explained by the ring-shaped maximum of the lateral temperature gradient, measured with BCECF.

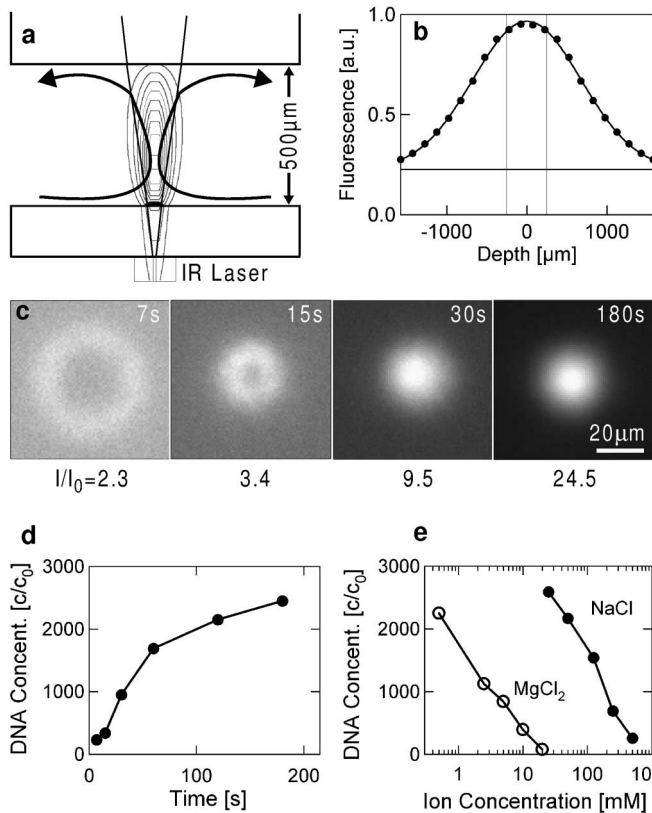


FIG. 3. Strong thermophoretic trapping of DNA. (a) Infrared heating is applied from a divergent beam in a 500  $\mu\text{m}$  thick chamber. (b) The fluorescence focus detects across the whole chamber, given by vertical lines. (c) Strong trapping of DNA is achieved and initially ring-shaped as imaged with fluorescence of a DNA stain. (d) The concentration of trapped DNA is increased more than 1000-fold, reaching an equilibrium within 180 s. (e) The salt dependence of trapping reflects the salt dependence of thermophoresis.

assume that DNA concentration is constant below  $d$ , we infer from the fluorescence intensity  $I/I_0$  an enhancement in concentration of  $c/c_0 = I/I_0 \times d/d_0 = 60$ .

The ring geometry can be understood from thermophoretic repulsion. We measure a radial temperature distribution [Fig. 2(e)] from cold and a hot fluorescence images of a BCECF-filled chamber. The shape of the temperature profile across the chamber is expected to be similar at different radial positions although the convection will distort it slightly. Thus the averaged horizontal temperature gradient is a measure of the horizontal temperature gradient near the chamber wall. The latter determines the thermophoretic velocity which depletes the accumulated DNA into a ring structure against the convergent flow [22] [Fig. 2(e)].

We estimate that the DNA does not melt. We measure an average chamber temperature of 80  $^{\circ}\text{C}$ ; the temperature of the trapped DNA is 42  $^{\circ}\text{C}$  as inferred from the increase of SYBR fluorescence as the heating is switched off. The low DNA temperature can be explained from its position near the cooler chamber wall. Melting of DNA is not expected, since the melting of DNA of this size begins at

85  $^{\circ}\text{C}$  with slow kinetics of 100–1000 s [23], whereas a convection cycle takes 5 s [24].

*Efficient thermophoretic trapping.*—We achieve strong trapping of DNA comparable to expectations from Eq. (2) by increasing the chamber thickness to  $d_0 = 500 \mu\text{m}$  (Fig. 3). Infrared heating is now applied from below directly out of a fiber (single mode, NA = 0.16, PL-7324-FC-2, Thorlabs) as given in Fig. 3(a). The theoretical temperature distribution is shown [Fig. 3(a), spacing 10 K]. The same 5.6 kbp DNA is used at a concentration of 0.5 nM and stained with YOYO [25] in a TRIS buffer (20 mM TRIS, 20 mM boric acid, 50 mM NaCl, 0.5 mM EDTA, pH 7.8). Images are now taken 2 s after switching off the heating laser to avoid blurring lensing from the temperature gradients.

Under these conditions, DNA is trapped to a point geometry with an intensity increase of  $I/I_0 = 24.5$  after 180 s [Fig. 3(c)]. Trapping begins with a rudimentary ring geometry at very early stages. The axial temperature gradients are obviously dominating the final equilibrium. The fluorescence is still averaged across the chamber [Fig. 3(b)]. From the convection, we estimate an accumulation height of about  $d = 5 \mu\text{m}$  and derive the concentration increase  $c/c_0 = I/I_0 \times d/d_0$  to be 2450-fold after 180 s [Fig. 3(e)]. It increases the DNA concentration of a typical plasmid size from 0.5 nM well into the  $\mu\text{M}$  concentration range within a microscopic spot of the dimensions of a cell.

To show that DNA molecules are not merely trapped by entangling or melting, we measure the diffusion coefficient of the accumulated DNA by fitting the diffusion of DNA with Gaussians after heating. We find a diffusion constant of single DNA molecules with  $D = 4.5 \times 10^{-8} \text{cm}^2/\text{s}$  in agreement with literature [19]. This indicates that single DNA molecules have been accumulated.

We study both thermophoresis and trapping with elevated salt concentrations. Thermophoresis of DNA is not detectable with 500 mM NaCl ( $D_T < 0.01 \times 10^{-8}/\text{s K}$ ) using the method described (Fig. 1). Thermophoresis also vanishes for 20 mM MgCl<sub>2</sub>. The DNA stain does not change its characteristic under these salt concentrations and a slightly more flexible DNA should not affect thermophoresis [10]. This salt dependence is consistent with a model of thermophoresis based on interfacial tension in the Debye layer [26]. Since the addition of 500 mM NaCl or of 20 mM MgCl<sub>2</sub> efficiently quenches trapping [Fig. 3(e)], we consider this as further proof that the trapping is driven by thermophoresis.

Thermophoresis until now was not considered for microfluidics or microarrays. Large temperature gradients of more than  $10^4 \text{K}/\text{cm}$  across water are achievable. Both dielectrophoresis [6] and optical tweezers [5] fail in manipulating DNA or proteins. Note that we can also trap polystyrene beads (200 nm, 1:100 dilution, F-8767, Molecular Probes) with a concentration ratio of  $c/c_0 = 230$  in the 50  $\mu\text{m}$  chamber configuration.

Thermophoretic trapping might bridge the concentration gap in prebiotic evolution. A main requirement in prebiotic studies of self-replicating systems and prebiotic metabolisms [3] are high concentrations of reaction partners. Taking the concentrations from a primordial soup results in kinetics much slower than the  $500 \times 10^6$  years which the earth apparently needed to develop first cellular organisms [4]. Proposed mechanisms such as evaporation of ponds, surface-active minerals, or concentration from eutectic freeze-out are not considered very persuasive [3,4].

We propose that hot and porous stones in a cold ocean could give rise to single or cascaded thermophoretic trapping cells. Heating spots could be formed by high thermal conductivity inclusions in the stone. The salinity of present day oceans reaches NaCl concentrations of 600 mM, much higher than the environment within living cells (150 mM) and likely to quench thermophoresis of biomolecules. Yet other scenarios of the origin of life argue towards lower salt concentrations, although the salinity of early oceans is under debate [27]. Since trapping is exponentially stronger for longer polymers [Fig. 1(d)], an evolutionary pressure towards more complex molecules is established. The temperature cycling inherent in the convection flow matches melting and annealing cycles of self-replication [28] with efficient cycling times in the second time scale. The trapping at a surface would be compatible with prebiotic reaction schemes at a catalyzing surface [29]. All these points make thermophoretic trapping an interesting new approach to prebiotic evolution which was not yet considered or discussed.

To conclude, we have found an efficient trapping mechanism in solution through the interplay of convection and thermophoresis. We demonstrated trapping of plasmid-sized DNA into microscopic volumes and quantified the thermophoresis of DNA. Thermophoretic trapping has interesting prospects in microfluidics and gives new clues to prebiotic evolution.

We thank Werner Köhler and Steve Arnold for discussions. Richard P. Haugland, Molecular Probes, helped in finding a temperature-sensitive dye. D. B. was supported by the Emmy Noether Program of the Deutsche Forschungsgemeinschaft.

---

\*Email address: mail@dieterb.de

- [1] C. Ludwig, Sitzber. Akad. Wiss. Wien, Math.-Naturw. Kl. **20**, 539 (1856).
- [2] C. Soret, Arch. Geneve **3**, 48 (1879).
- [3] G. Zubay, *Origins of Life on the Earth and in the Cosmos* (Academic Press, San Diego, 2000).
- [4] S.J. Mojzsis, R. Krishnamurthy, and G. Arrhenius, in *The RNA World*, edited by R. F. Gesteland, T. R. Cech, and J. F. Atkins (Cold Spring Harbor Laboratory Press, New York, 1999).
- [5] S. Katsura, K. Hirano, Y. Matsuzawa, K. Yoshikawa, and A. Mizuno, *Nucleic Acids Res.* **26**, 4943 (1998).
- [6] T. Schnelle, T. Muller, G. Gradl, S.G. Shirley, and G. Fuhr, *Electrophoresis* **21**, 66 (2000).
- [7] J.C. Maxwell, *Collected Papers II* (Cambridge University Press, Cambridge, 1879), pp. 681–712.
- [8] P.S. Epstein, *Z. Phys.* **54**, 537 (1929).
- [9] S.R. de Groot and P. Mazur, *Non-equilibrium Thermodynamics* (North-Holland, Amsterdam, 1969).
- [10] M.E. Schimpf and S.N. Semenov, *J. Phys. Chem. B* **104**, 9935 (2000).
- [11] M. Giglio and A. Vendramani, *Phys. Rev. Lett.* **38**, 2 (1977).
- [12] W. Köhler and P. Rossmannith, *J. Phys. Chem.* **99**, 5838 (1995).
- [13] C. Debuschewitz and W. Köhler, *Phys. Rev. Lett.* **87**, 055901 (2001).
- [14] J.C. Giddings, M.E. Hovingh, and G.H. Thompson, *J. Phys. Chem.* **74**, 4291 (1970).
- [15] M.E. Schimpf and J.C. Giddings, *J. Polym. Sci. B, Polym. Phys.* **27**, 1317 (1989).
- [16] K. Clusius and G. Dickel, *Z. Phys. Chem. Abt. B* **44**, 397 (1939).
- [17] K. Clusius and M. Huber, *Z. Naturforsch. A* **10a**, 230 (1955).
- [18] Fiber coupled solid state laser, FOL1402PJX-317, Furukawa. Its center wavelength of  $\lambda = 1480$  nm yields an intensity attenuation length in water of  $400 \mu\text{m}$ . The laser is focused with numerical aperture of 0.19 to a Gaussian profile of width  $\sigma = 38 \mu\text{m}$ .
- [19] A. Pluen, P.A. Netti, R.K. Jain, and D.A. Berk, *Biophys. J.* **77**, 542 (1999).
- [20] M.E. Schimpf and J.C. Giddings, *J. Polym. Sci. B, Polym. Phys.* **28**, 2673 (1990).
- [21] For much shorter DNA (27 bp,  $10 \mu\text{M}$ ), we measure  $c/c_0 = 97\%$  and  $D = 36 \times 10^{-8} \text{ cm}^2/\text{s}$ , and therefore  $S_T = 0.013 \text{ K}^{-1}$  and  $D_T = 0.45 \times 10^{-8} \text{ cm}^2/\text{s K}$ . The found  $D_T$  is independent of the DNA length as expected from scaling arguments of polymer thermophoresis. From a temperature gradient of 50 K only a depletion of  $c/c_0 = 0.52$  is expected due to the difference in  $D$  [Fig. 1(d)].
- [22] The ring geometry can be changed to a point geometry by defocusing the heating spot width from  $\sigma = 9$  to  $40 \mu\text{m}$ . Now the horizontal temperature gradient is smaller and cannot force the ring structure, and accumulation is due to only the axial temperature gradient in the stagnation point of the convection.
- [23] M.T. Record and B.H. Zimm, *Biopolymers* **11**, 1435 (1972).
- [24] Trapping is reduced to 30-fold using half the heating power with chamber temperatures of  $60^\circ\text{C}$  and DNA temperatures of  $35^\circ\text{C}$ .
- [25] S. Gurrieri, S.B. Smith, K.S. Wells, I.D. Johnson, and C. Bustamante, *Nucleic Acids Res.* **24**, 4759 (1996).
- [26] R. Piazza and A. Guarino, *Phys. Rev. Lett.* **88**, 208302 (2002).
- [27] L.P. Knauth, *Nature (London)* **395**, 554 (1998).
- [28] H. Kuhn, *Naturwissenschaften* **63**, 68 (1976).
- [29] G. Wächtershäuser, *Proc. Natl. Acad. Sci. U.S.A.* **87**, 200 (1990).